Some New Features of the Dual CESE solver in LS-DYNA and its applications

Grant Cook Jr[1], Zeng-Chan Zhang[2]

[1]LST, an ANSYS Company, Livermore CA 94551, USA
[2]LST, an ANSYS Company, Livermore CA 94551, USA

Abstract

In this paper, we briefly review the dual-CESE solver that is an improved version of the regular CESE solver. For instance, compared to the regular CESE solver, it is more accurate and stable, and particularly more stable for triangle (2D) /tetrahedral (3D) meshes, all while maintaining the core features of the CESE method. Some of the new features of the Dual CESE solver in the R15 release will then be explained. Probably the most significant new capability is the addition of the multiphase phase-change solver to the suite of dual CESE solvers. An implementation of a “point-source” method of injecting a gas flow inside the volume of the fluid mesh is also new in R15. Several examples will be given showing how to use the new capabilities of this Dual CESE solver. Also, some significant multiphase capabilities that were new with the R14 release of LS-DYNA are also demonstrated. Other features include several different kinds of time-history outputs from the dual CESE solver that are accessed through the binout mechanism in LSPP. The most recent such feature in R15 is the binout time history interface for the plotting of drag, lift, and related variables; this is now supported in LSPP4.11. LSPP4.10 also supports the time history binout output from all of the Dual CESE solvers, including the new (R15) phase-change solver. An important upgrade for the R15 version of LS-DYNA is a more robust material erosion FSI capability for all dual CESE solvers. Finally, new in R15 are boundary conditions for the single-phase Dual CESE solvers that have been introduced to help with aerospace-type applications.

1 Introduction

The main purpose of the CESE-type compressible flow solvers in LS-DYNA is to permit fluid-structure interaction (FSI) calculations where the fluid and structural solvers are coupled together. Based upon adequate mesh resolution, these compressible flow solvers capture shocks with high accuracy, and at the same time handle low speed flow features. With a structural coupling that includes the ability to deal with material erosion, a wide range of applications are now accessible.

This paper will focus on the R15 additions to the Dual CESE compressible flow solver. These additions include: a phase-change multiphase solver, a point-source gas injection method, drag and lift calculation with the immersed boundary method (IBM) FSI solvers, time history output for the new solvers, major corrections to the material erosion FSI method, and a set of new boundary conditions.

Before describing these additions, it is essential to understand why users should care about the Dual CESE solver.

The motivation for the invention and development of the Dual CESE solver in LS-DYNA began when some shortcomings became evident in the older CESE solver. The primary issue was the sensitivity of the CESE method to meshes that have large jumps in element size, or even difficulties with some triangle (2D) and tetrahedral (3D) meshes. While overcoming these mesh sensitivities, at the same time improved accuracy is obtained. In spite of these improvements, it is still recommended that the mesh be constructed with smoothly varying element sizes. The net effect is that the Dual CESE method has improvements related to accuracy and robustness compared with the older CESE method. Significantly, the Dual CESE numerical method maintains all of the strengths of the basic CESE numerical method.

What are these features that originally led us to the CESE approach?

First, CESE was developed for modeling systems of conservation laws that are typical of models in compressible fluid dynamics. The numerical technique is called the Conservation Element/Solution Element (CESE) method. It is a novel numerical framework for conservation laws with many non-traditional features, including treating space and time in a unified way, introducing separate conservation elements (CE) and solution elements (SE), and use of a novel shock capturing strategy that avoids the use of a Riemann solver. The CESE method has been used to solve many types of flow problems, such as detonation waves, shock/acoustic wave interaction, cavitating flows, supersonic liquid jets, and chemically reacting flows.

In LS-DYNA, the CESE method has been extended to also solve fluid-structure interaction (FSI) problems. It does this with two approaches. The first approach solves the compressible flow equations on an Eulerian mesh while the structural mechanics is solved on a moving mesh that moves through the fixed CESE mesh. In the second approach, the CESE mesh is morphed in a fashion such that its FSI boundary surface matches the corresponding FSI boundary surface of the moving structural mechanics mesh. This second approach is more accurate for FSI problems, especially with boundary layers flows. But the moving mesh method is much more expensive, and this expense grows with the number of CESE mesh elements.

Now turning to the dual CESE solver, it is also intended for use as a compressible flow solver that is based upon a modified Conservation Element/Solution Element (CESE) method that is still intended for systems of conservation laws.

In LS-DYNA, the dual CESE solver also includes fluid-structure interaction (FSI) capabilities of the moving mesh and immersed boundary types. Another goal of the new dual CESE solver as compared with the older CESE solver was to allow each FSI approach (or fixed mesh CFD solver) to be employed in different subregions of the fluid mesh in the same problem. As of this writing, this is still not operational.

While most of the solvers in the LS-DYNA CESE solver have been reimplemented in the Dual CESE solver, not all of them were ported. In particular, it is unclear if the CESE chemically-reacting flow solver will be ported to the Dual CESE solver.

There are many solvers implemented in LS-DYNA with the Dual CESE flow solver method, especially several multiphase solvers. To support these, many new types of EOSes have been added. Also, for modeling condensed-phase explosives, several types of single-step reaction rate models have been implemented.

The modeling approach of these multiphase solvers is based on a hybrid formulation, i.e., a mixture of a multiphase formulation and an augmented Euler formulation. It is designed for the numerical simulation of condensed-phase explosives. It can handle two miscible components, namely the reactant and the products of reaction, and one inert immiscible component, such as the confiner in the case of the rate-stick.

Notable features of this hybrid model include that it can provide the accurate recovery of the temperature field across all components, and also can sustain large density differences across material interfaces. It can accommodate realistic EOS and arbitrary (pressure or temperature-based) reaction-rate laws.

The main applications of these multiphase solvers include the numerical simulation of condensed-phase commercial- and military-grade explosives. Of particular interest is the propagation of detonations in compliantly confined charges (rate-stick-type problems) and the sensitization of commercial explosives by means of collapsing micro-balloons.

For example,
• simulation of combustion and transition to detonation of condensed phase explosives
• propagation of detonations in compliantly confined charges (rate-stick-type problem)
• sensitization simulation of commercial explosives by means of collapsing micro-balloons
• shock-induced cavity collapse in liquid explosives

Currently available EOSes include:
• Mie-Gruneisen type EOSes: Ideal-gas EOS, JWL EOS, and Cochran-Chan EOS
• generalized Van der Waals EOS, including standard Van der Waals EOS and a stiffened gas EOS

Currently available reaction rate laws include:
• Ignition and Growth (I&G) model
• Simplified Ignition and Growth (I&G) model
• Simple pressure-dependent reaction rate law

We also implemented a solver for one of the hybrid formulation reduced models, i.e., a two-phase model (a 5-equations model). In this model, only two immiscible materials can be included.

The multiphase cavitation model from the LS-DYNA CESE solver has also been ported to the Dual CESE solver.

Finally, a new multiphase phase-change solver is added to the Dual CESE solver with the R15 release. It will be discussed later.

All of these multiphase solvers in the Dual CESE solver have 3D, 2D axisymmetric, and 2D versions. All of them also have FSI capabilities with the immersed boundary method (IBM) FSI technique. This includes a material erosion capability that allows modeling of damage computations in the presence of energetic materials.

2 R15 numerical examples: Phase-change solver

In R15, a new phase transition multiphase model is added. In this model, the thermochemical relaxation algorithm is adapted [1] and it is fast compared with the common iterative procedure used in phase-change solvers. In this model, a multicomponent fluid can be considered, i.e., liquid, vapor and air, and the general 'Nobel-Abel Stiffened Gas' (NASG) [1-2] EOS is used. Of course, the popular ideal gas law EOS is included as a special case of this NASG EOS. The main application areas of this model include cavitating, evaporating, and condensing two-phase flow simulations. In the following, we will show some application examples.

2.1 Evaporating liquid jet

This example is adapted from ref [1] to validate our implemented model. In this example, the simulation is of an evaporating liquid jet in a cryotechnic rocket engine during ignition phase. The flow consists of a coaxial liquid oxygen jet surrounded by a high-speed hydrogen flow, injected in conditions above the saturation point of the inner oxygen core, which then evaporates whilst being destabilized (see Fig. 1). The inlet boundary conditions are:

1. central flow (liquid oxygen): at temperature T=100 K, injecting velocity V=30 m/s and pressure P=3 MPa.
2. peripheral flow (gaseous hydrogen): at temperature T=150 K, injecting velocity V=200 m/s and pressure P=3 MPa.

A reflective boundary condition is used along the nozzle wall, while a background pressure P=3 MPa is applied at all other open boundary surfaces. The mesh used in this simulation consists of 554700 quadrilateral elements, and Fig. 2 shows three snapshots of the vapor (y2) contours, illustrating the evaporating liquid jet configurations; it's very similar to the results in ref [1].

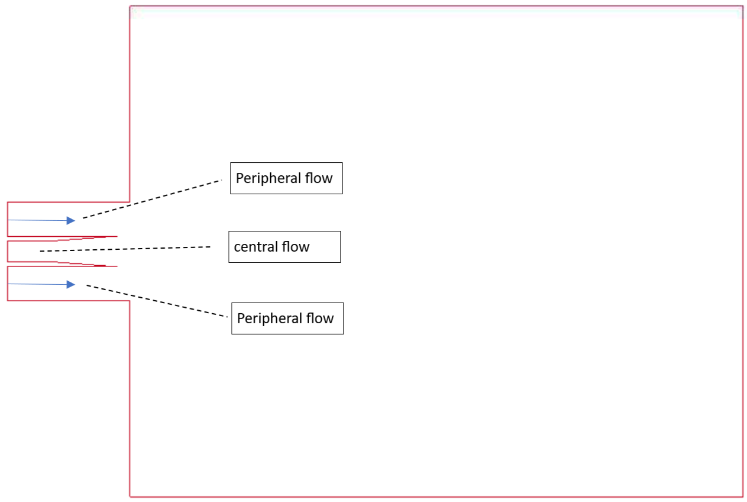

Fig. 1: sketch of the liquid jet evaporating in a nozzle

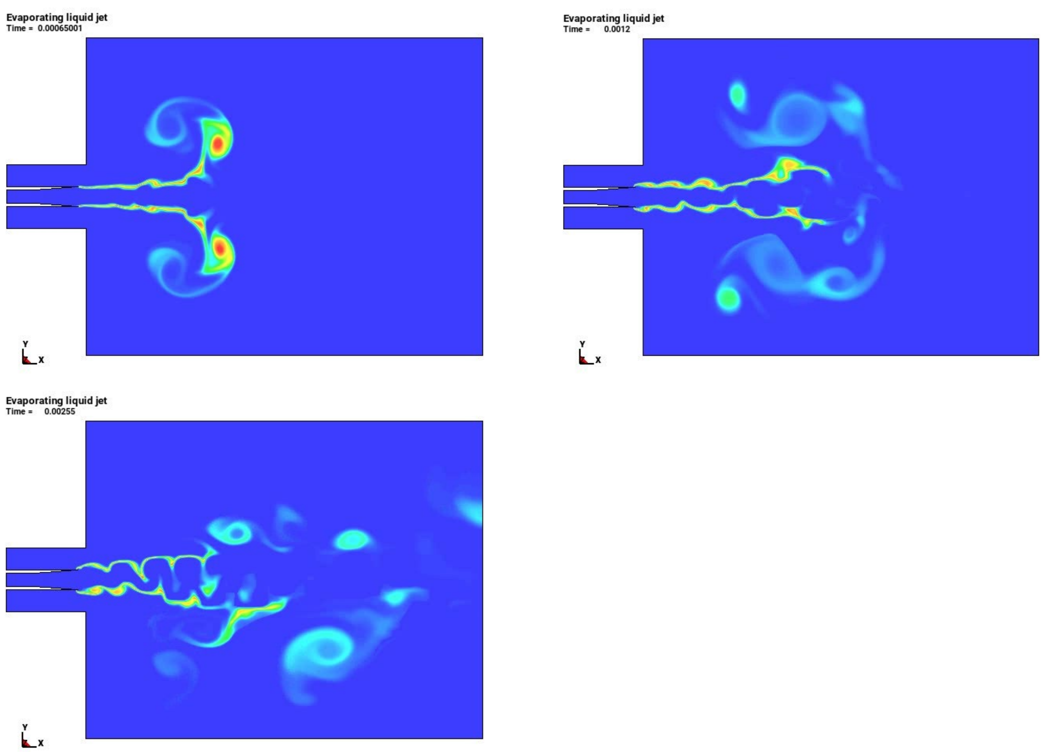

Fig. 2: mass fraction of vapor (y2) contours at three times during the liquid jet evaporating process

2.2 Fuel tank impact/penetrated by a bullet

Our Dual CESE phase-change model is extended to be coupled with the LS-DYNA structural solver in order to solve more general fluid/structure interaction problems with phase transitions. Here this capability is used to simulate a fuel tank (filled with water) impacted or penetrated by a bullet. Fig. 3 gives the sketch of this problem. A fast-moving bullet collides with and penetrates the right wall of the tank first, then it moves through the tank at high speed. Behind the bullet a cavitation region develops because of the fluid perturbations caused by the fast-moving bullet. At the same time the tank walls will deform because of the fluid rush, and some small regions of cavitation can be seen near the tank walls. Fig. 4 shows two snapshots during the time when the bullet is moving inside the tank (only a middle slice is shown for clarity).

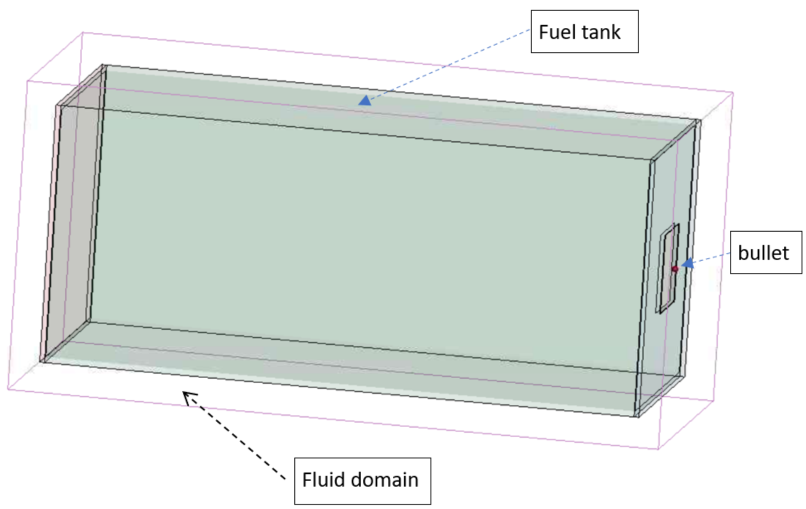

Fig. 3: sketch of fuel-tank problem

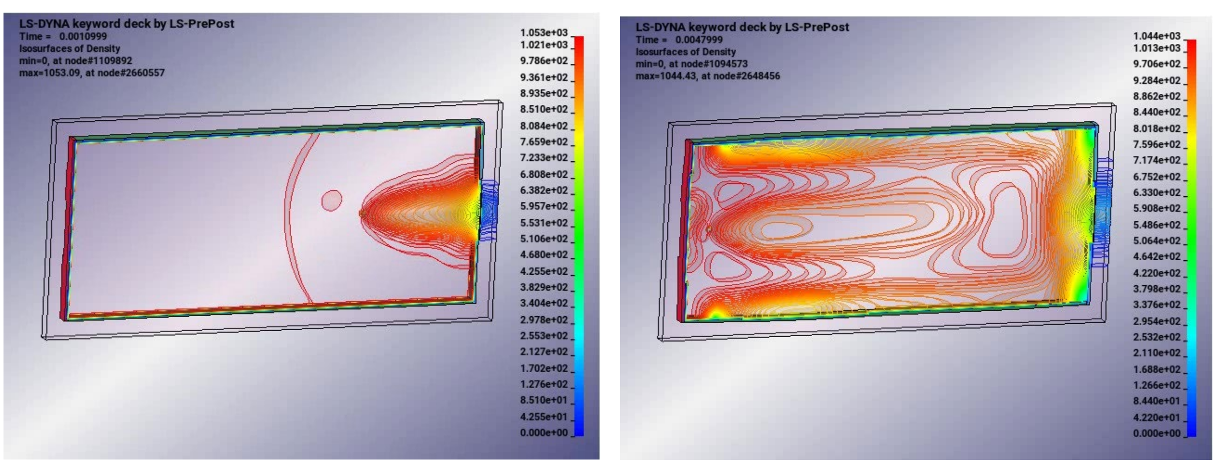

Fig. 4: Fluid density contours at two times during the bullet fast moving inside the fuel-tank

3 R15 numerical examples: Point-source flow injection

3.1 Folded-bag deployment

Based on users' requirements, a new point source capability has been added in R15 to CFD and two-phase flow solvers (including fluid/structure interaction (FSI) solvers). This capability is especially useful in folded-bag deployment simulations and will give users a more flexible way to specify the bag inlet boundary conditions. In this point-source option, the users can specify the regular flow variables (just like our prescribed boundary condition) or give a mass flow rate plus other suitable flow conditions. The location of the point source can be defined to be at any point inside the fluid domain. Of course, it is better if this point is close to the fluid element center for better accuracy. Here, we want to emphasis that this point-source capability is also available for two-phase multiphase cases, e.g., the point-source fluid and the surrounding fluid can be defined as two different fluids, each using a different EOS. As a simple demonstration, one of our older folded-bag deployment examples is reproduced by using the point-source capability. Fig. 5 shows the point-source location (near the inflow tube exit), and Fig. 6 shows three flow field snapshots during the bag deployment process.

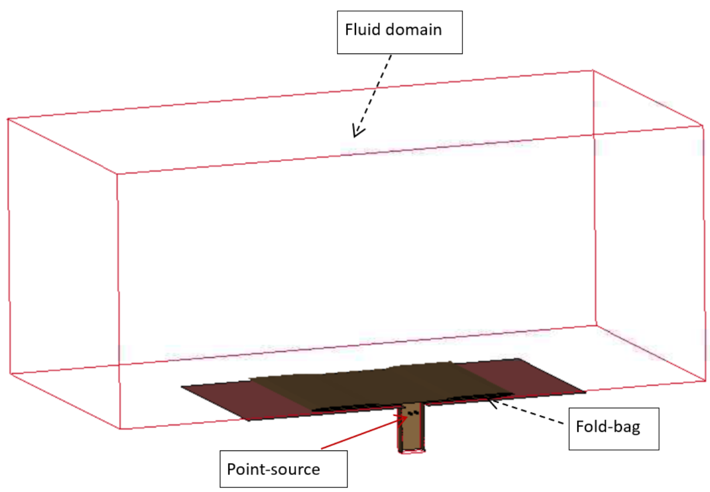

Fig. 5: sketch of fold-bag deployment

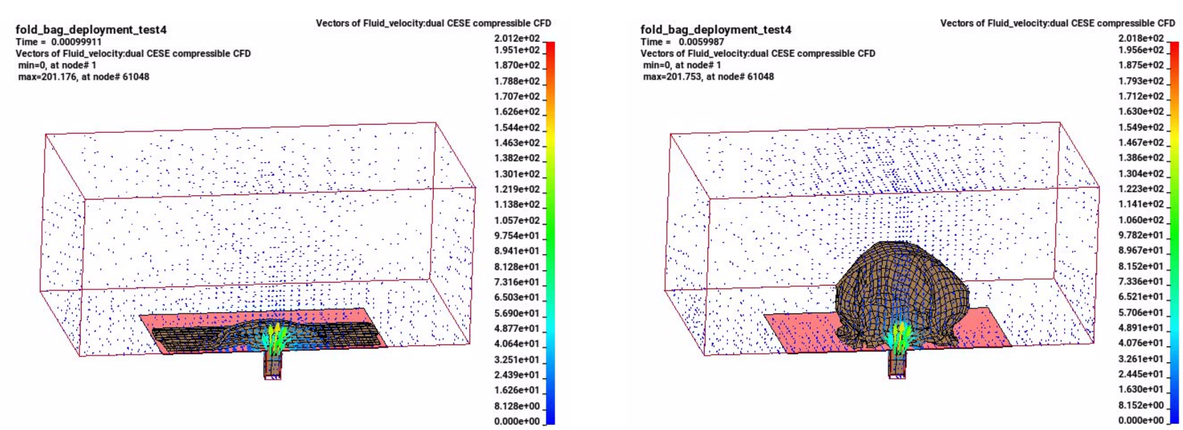

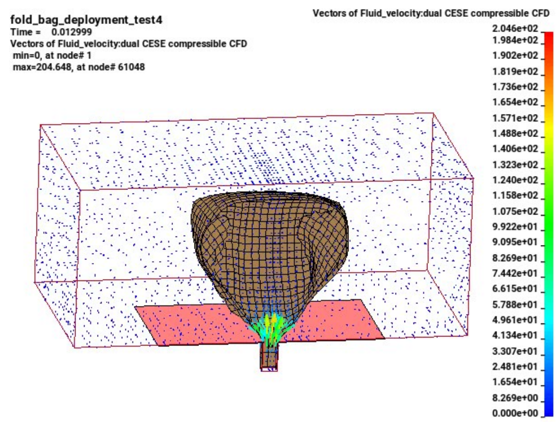

Fig. 6: fluid velocity and bag deployment process

4 Further R15 features: Material erosion FSI improvements

As mentioned earlier, the Dual CESE immersed boundary method (IBM) FSI solvers allow for material erosion to occur in the structural parts undergoing erosion or material failure. These solvers also allow for some of the structural parts to be excluded from the FSI interaction. This is desirable when a given part has little interaction with the flow field, or when it is expedient for the sake of calculation speed to remove as many parts as possible from the FSI interaction. Until recently, if material erosion was occurring in parts excluded from FSI interaction calculations, the calculation would halt, or get erroneous results. With R15 (and also R14.1) the material erosion FSI calculation has been extended to take into account this rare situation. Another error was the incorrect updating of IBM FSI information when a material erosion event occurs. This has also been fixed in R15 and R14.1, but not in earlier versions of LS-DYNA. Please contact us if this is an issue for your use of the Dual CESE solver.

5 Further R15 features: Drag and lift calculation with the Dual CESE IBM FSI solvers

Another significant addition to the R15 Dual CESE solver is the ability to output time histories of drag, lift, and related quantities to the binout file using the **`*DUALCESE_DATABASE_HISTORY_DRAG_LIFT`** card. This feature is especially designed to work in IBM FSI calculations where structural parts are breaking apart and forming new pieces. The way this works is that the Dual CESE solver automatically computes the topologically-separate pieces of all structural parts that are active in the FSI calculation. Due to material erosion during IBM FSI simulation, each of the structural pieces for which drag and lift are being computed can have different starting and stopping times for the binout output of the drag-related variables. Here are the possible reasons:

1) A piece can break off from another structural piece at any given time during the simulation
2) A structural piece can completely erode away (disappear) from the problem.

Plotting these drag-related variables is now possible with the current version of LSPP4.11, using its binout interface. Fig. 7 is an example of plotting the drag coefficient for four of the pieces in a Dual CESE IBM FSI calculation. These are all shell pieces. As can be seen, piece 5 disappears from the problem at an early time. In this case, it is due to programmed failure (erosion) of the entire shell part to which piece 5 corresponds. Also, piece 7 is created at time 3.0e-3 seconds, and this is due to a region of a shell piece breaking off from its parent piece. See Fig. 8 for the other LSPP4.11 windows that show how the binout time history plotting was initiated.

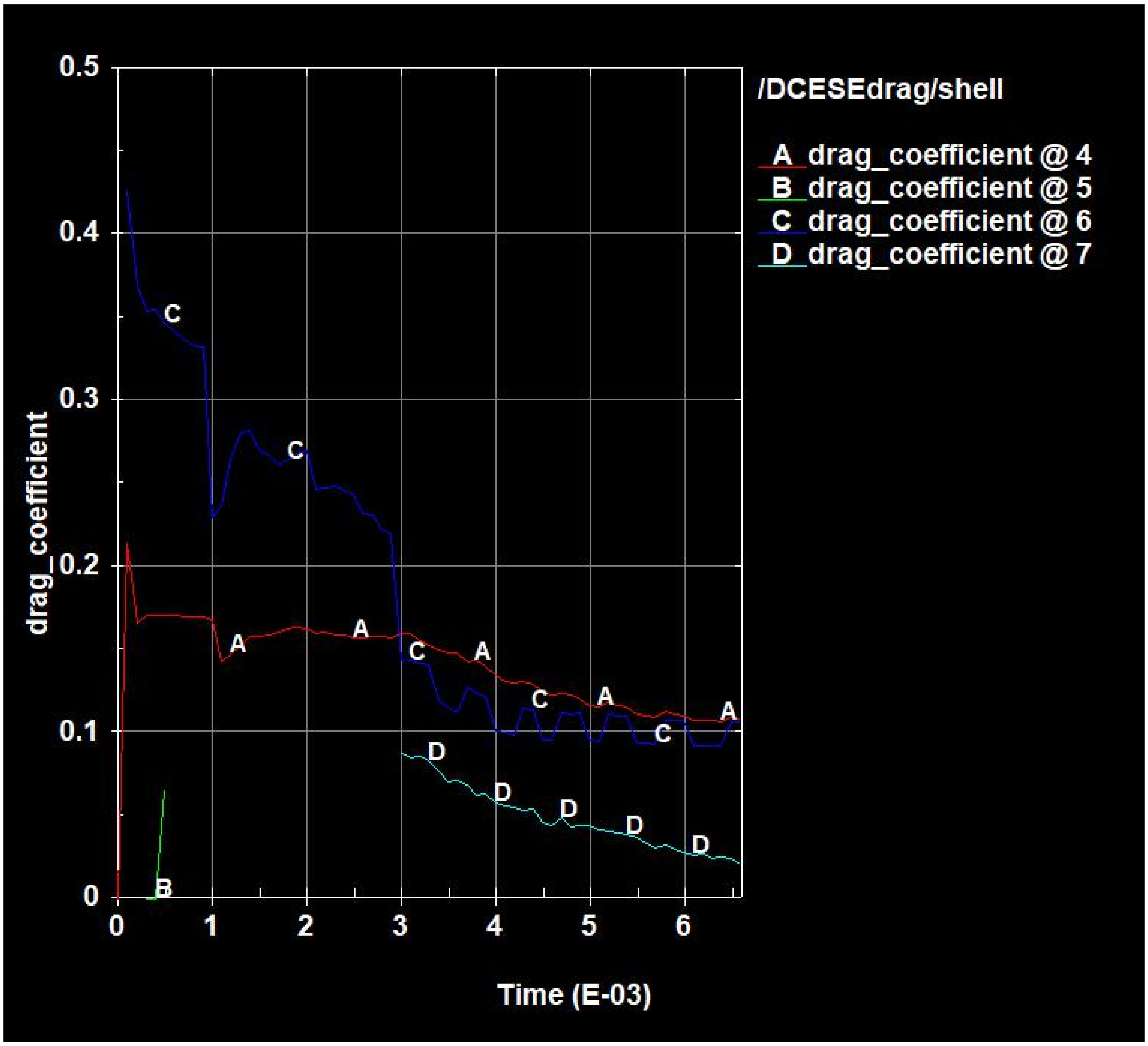

Fig. 7: drag coefficient time history plot for several structural “pieces” (from an IBM FSI calculation)

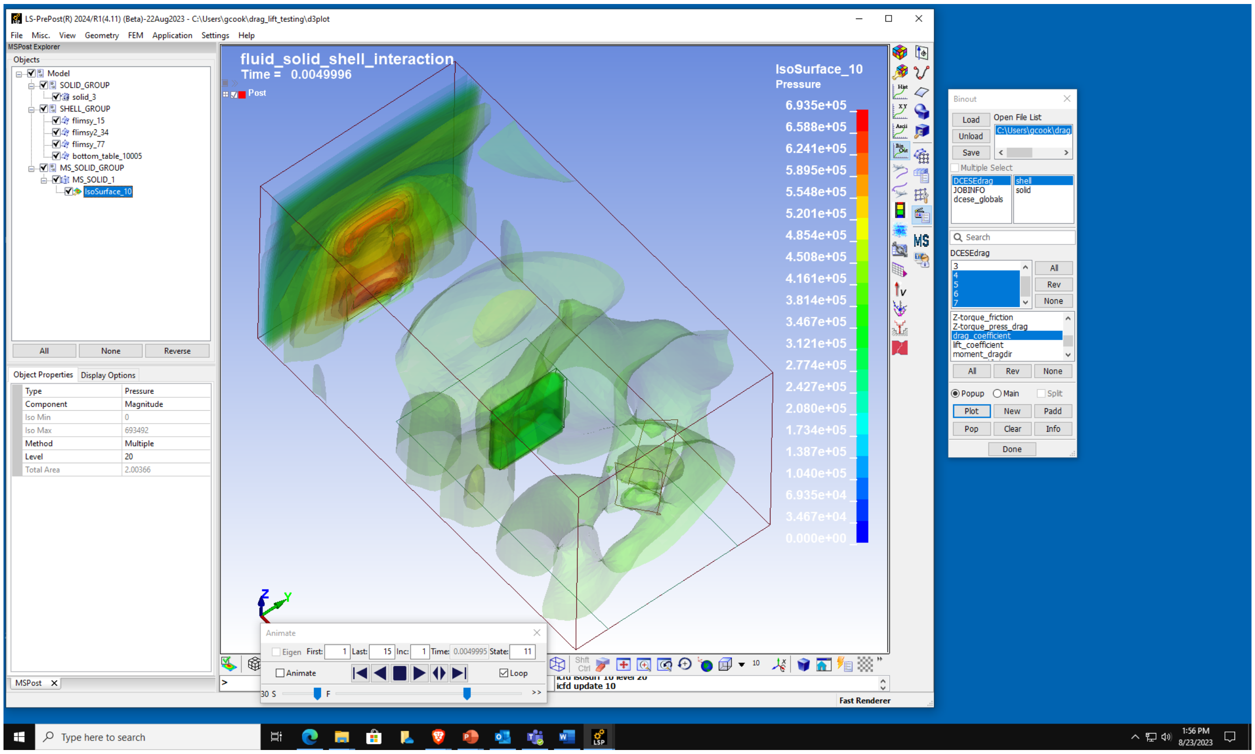

Fig. 8: IBM FSI calculation showing isocontours of fluid pressure, and the binout window used to select the drag coefficient time histories that are plotted in Fig. 7.

One limitation of this new drag/lift capability is that it was implemented only for the Dual CESE IBM FSI solvers. That is, at present, no drag calculations are available with the Dual CESE moving mesh method FSI solvers, or the non-FSI dual CESE solvers.

6 Further R15 features: Time history plotting using binout output from the Dual CESE solvers

The following keywords initiate time history output to the binout file for all Dual CESE solvers, and for the new phase-change multiphase solver in particular. Support for these time histories starts with LSPP4.10.

```
*DUALCESE_DATABASE_HISTORY_ELEMENT_SET
*DUALCESE_DATABASE_HISTORY_GLOBALS
*DUALCESE_DATABASE_HISTORY_NODE_SET
*DUALCESE_DATABASE_HISTORY_POINT_SET
*DUALCESE_DATABASE_HISTORY_SEGMENT_SET
```

Fig. 9 shows an LSPP time history plot of temperature on an element set for the Dual CESE phase-change multiphase solver. The simulation is of non-hydro nozzle cavitation.

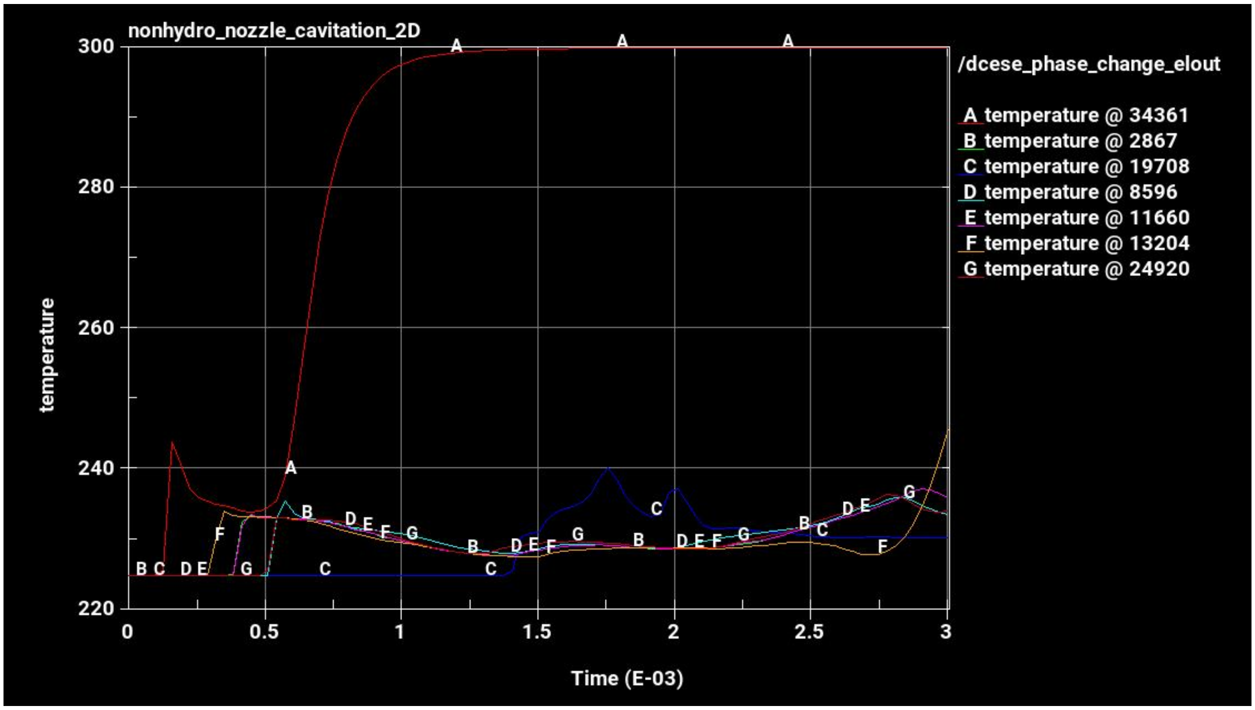

Fig. 9: temperature at selected elements in a non-hydro nozzle cavitation simulation computed with the new Dual CESE phase-change multiphase solver.

7 Further R15 features: New boundary conditions for the Dual CESE CFD solvers

Recently, we added several new boundary conditions for inlets and outlets that are appropriate for gas turbine and similar applications. These are documented in the R15 Vol. III keyword manual. These keywords provide the option for the user to specify Mach number, mass flow rate, etc. at the problem inlet, and to specify Mach number, mass flow rate or pressure at a problem outlet.

```
*DUALCESE_BOUNDARY_PRESCRIBED_INLET_MACHNUM
*DUALCESE_BOUNDARY_PRESCRIBED_INLET_PRESSURE
*DUALCESE_BOUNDARY_PRESCRIBED_INLET_MASSFLRATE
*DUALCESE_BOUNDARY_PRESCRIBED_OUTLET_FARFIELD
*DUALCESE_BOUNDARY_PRESCRIBED_OUTLET_PRESSURE
*DUALCESE_BOUNDARY_PRESCRIBED_OUTLET_MASSFLRATE
```

8 Multiphase R14 numerical examples

Some of the important multiphase Dual CESE capabilities that were introduced with the R14 release are highlighted in the following sections. Here we show results from four additional examples. To see other examples, please go to the '*dynaexamples.com/cese/dualcese*' website, the '*lsdyna.ansys.com/knowledge-base/cese/dual-cese*' website, or our ftp website at this location: '*ftp.lstc.com/anonymous/outgoing/gcook/DualCESE_examples*'. The examples available at this ftp site location are the only ones using the newer preferred keywords (the new approach introduced with R14).

8.1 Cavitation induced by needle movement in a nozzle

In the older LS-DYNA CESE solver, we implemented a cavitation model, i.e., Schmidt's homogeneous equilibrium model (HEM) [3], which is based on the acoustic speed of the mixture of liquid and vapor. This model is simple but contains the important characteristic information of cavitating flows. This cavitation model is very suitable for high-speed flows in small geometry, like diesel injection systems. This cavitation model was ported to the Dual CESE solver (starting from R14) and IBM FSI capabilities were also added. In the current example, a needle moves backward and forward periodically to automatically close and then open a fuel nozzle. During this process, some cavitation occurs inside the nozzle because of the needle perturbations. Fig. 10 shows three snapshots of the flow field (density) with needle movement inside the nozzle.

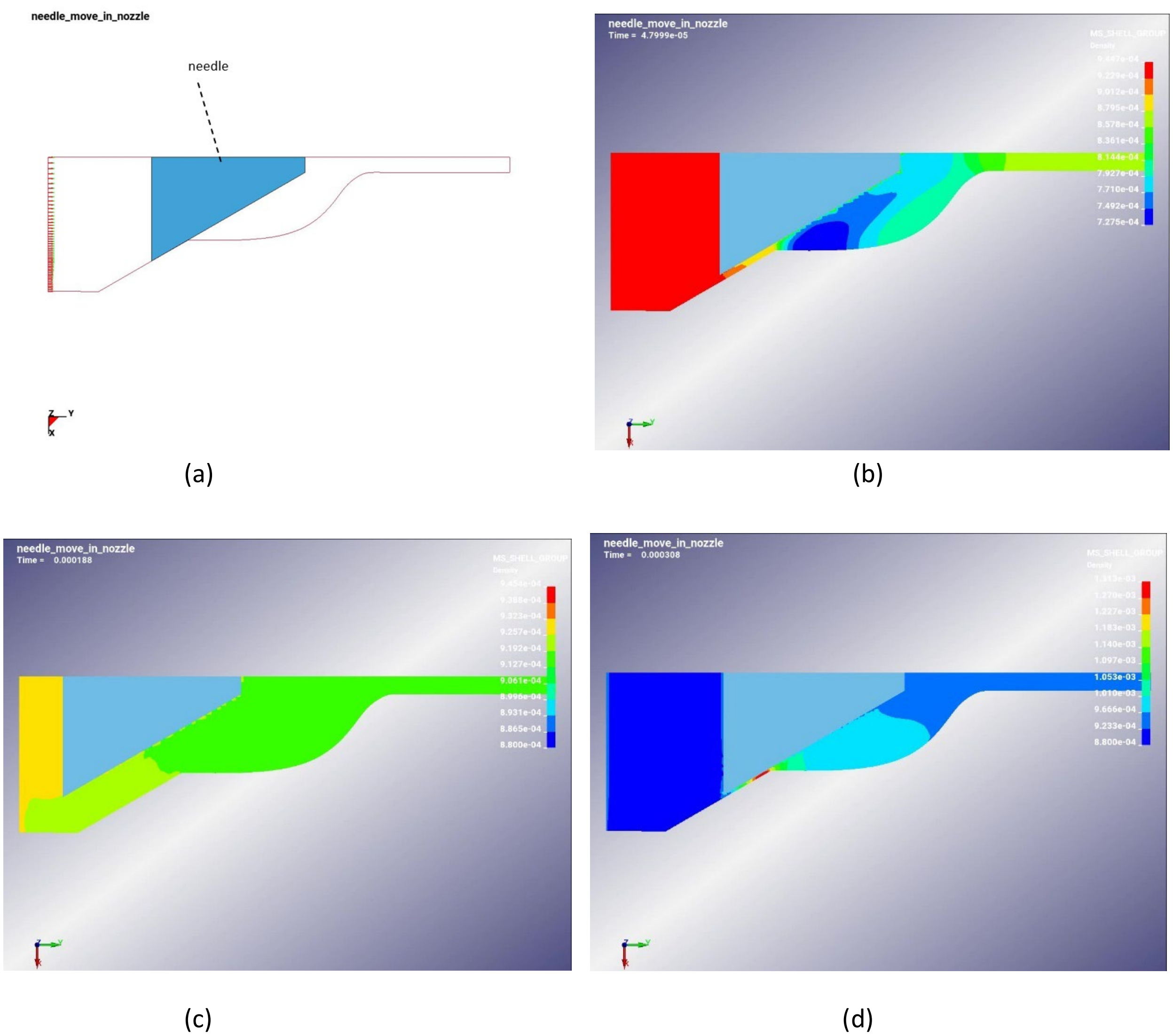

Fig. 10: fluid density contours at three times during needle motion back and forth inside a nozzle.

8.2 Cavitating flow in a 3D nozzle

In this example, the cavitation model, i.e., Schmidt's homogeneous equilibrium model (HEM) model is used. Fig. 11 shows the flow field after it reaches the steady state. It can be seen that cavitation forms behind the neck corner. Please note that the recently implemented phase-change model (available in R15) can also be used for cavitating flow simulations.

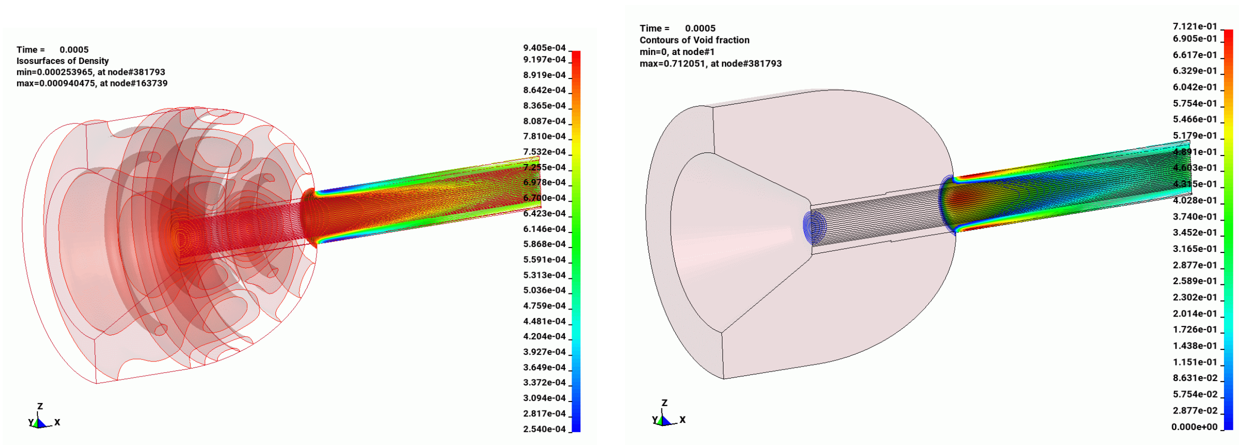

(a) (b)

Fig. 11: Density (a) and void fraction (b) contours of cavitating flows in a 3D nozzle.

8.3 Rate-stick in a cylinder container

In this example, the hybrid multiphase flow model is used. The hybrid multiphase model is implemented in the Dual CESE solver beginning with R14. This model incorporates the features of the augmented Euler and multiphase approaches [5]. It can handle three materials, including two of the mixture reactants (reactants & productions) and one inert material. A one-step reaction is assumed, and one of several reaction rate laws can be chosen, including the popular ignition and growth (I&G) reaction rate law. Available EOSes now include the general Mie-Grunisen type EOS (e.g., JWL, Cochran-Chan, etc.) and the generalized van der Waals EOS (including the stiffened gases EOS, etc.). This model targets condensed phase explosives, such as the propagation of detonations in compliantly confined charges, shock-induced cavity collapse in liquid explosives, etc. In the current example, condensed explosives are loaded in a cylinder container, and ignited by a booster at the left bottom of the container. Once the explosives are ignited, a detonation wave is formed and propagates through the slab of the reactive material to the right. The high pressure behind the detonation wave front forces the container to comply and deform. The explosive considered in this scenario is LX-17 and the Ignition and Growth (I&G) reaction rate law is assumed. Fig 12 shows three snapshots during this process.

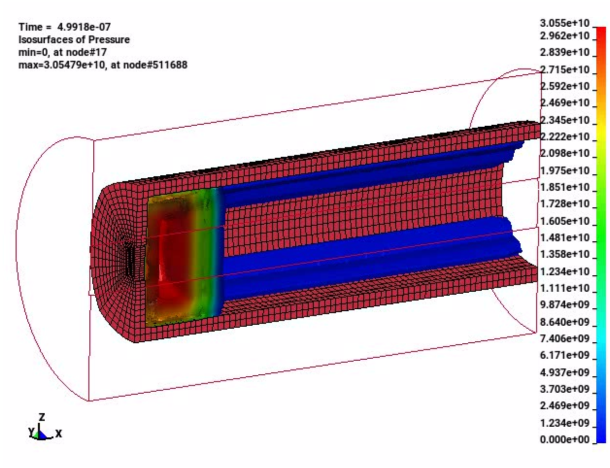

(a)

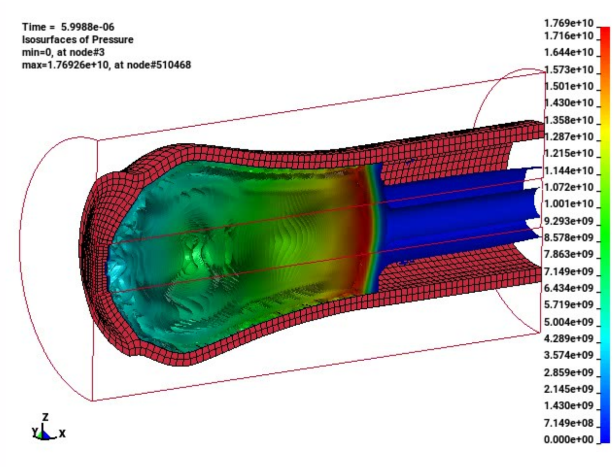

(b)

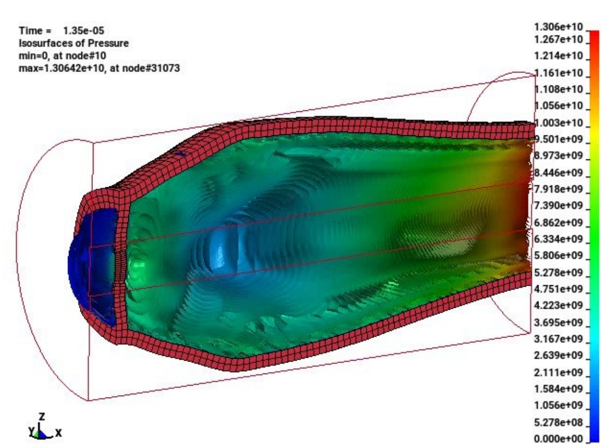

(c)

Fig. 12: Pressure contours and structure deformation of a rate-stick in a cylinder container

8.4 Shock bubble interaction with FSI

In this example, a two-phase model is used. It is a reduced model of the hybrid multiphase model where the mixture reactants are reduced to one inert material. Of course, no reaction will be considered, and it can handle only two immiscible materials. The available EOS is like that in the above hybrid multiphase model. In this test case, a left moving shock wave propagates and first hits a stationary bubble, which gains speed and loses its circular shape. After the shock wave hits the bubble, the circular pressure waves created keep moving forward and hit the structural panel causing its deformation. Fig. 13 shows the fluid field and structure deformation during this process.

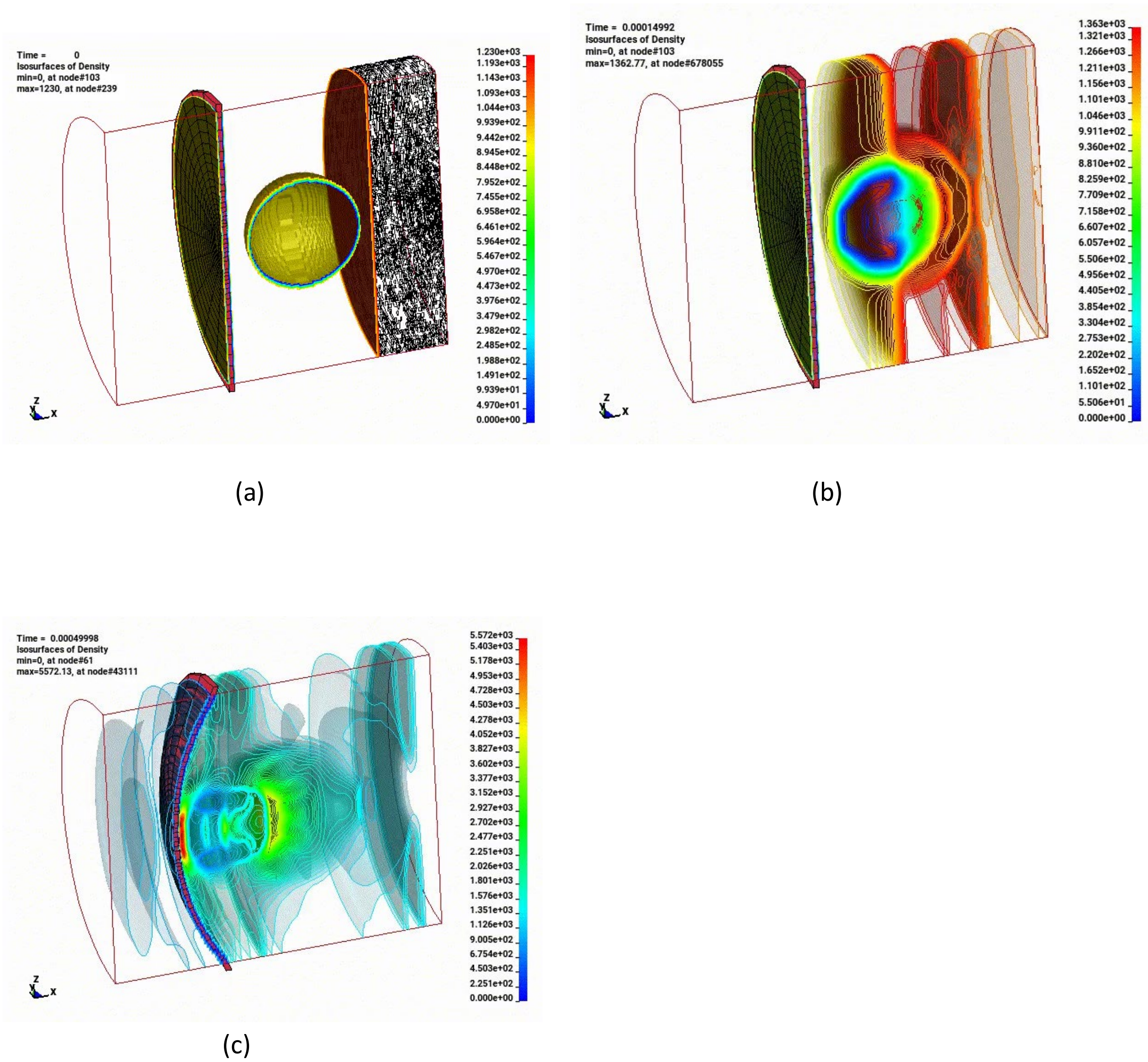

Fig. 13: Density contours and structure deformation of a shock-bubble-structure interaction

9 Summary

In this paper, after a brief review of the Dual CESE solver, the new features in LS-DYNA release R15 were presented. The addition of the multiphase phase-change solver to the suite of dual CESE solvers fills in an important gap in our multiphase capabilities. This is also true of the new “point-source” method for injecting a gas flow inside the volume of the fluid mesh. Calculation of drag, lift and related variables has long been requested. Time histories of these values are now output to the binout file with a new Dual CESE keyword card, but only in the IBM FSI solvers. More robust material erosion treatment in the IBM FSI was also mentioned. New single-fluid solver boundary conditions were also listed. Finally, it should also be mentioned that starting with LSPP4.10, users now have access to the Dual CESE Solution Explorer for setting up the Dual CESE portion of the input deck.

10 Literature

[1] Chiapolino, A., Boivin, P., Saurel, R., 'A simple and fast phase transition relaxation solver for compressible multicomponent two-phase flows', Computers & Fluids, Vol.150 (3) 2017.
[2] Le M´etayer, O., Saurel, R., The Noble-Abel Stiffened-Gas equation of state, Physics of Fluids 28 (4) 2016.
[3] Schmidt, D.P., Rutland, C.J., Corradini, M.L., "A Fully Compressible Two-Dimensional Model of Small, High Speed Cavitating Nozzles," Atomization Sprays Technology 9 (1999) 255-276.
[4] Michael, L., Nikiforakis, N., A hybrid formulation for the numerical simulation of condensed phase explosives, J. Comp. Phys. 316 (2016) 193-217.
[5] Allaire, G., Clerc, S., Kokh, S., A five-equation model for the simulation of interfaces between compressible fluids, J. Comput. Phys. 181(2) (2002) 577-616.